

Citation for published version: Zhao, P & Gu, C 2021, 'Water-Energy Nexus Management for Power Systems', IEEE Transactions on Power Systems, vol. 36, no. 3, pp. 2542 - 2554. https://doi.org/10.1109/TPWRS.2020.3038076

DOI:

10.1109/TPWRS.2020.3038076

Publication date: 2021

Document Version Peer reviewed version

Link to publication

© 2020 IEEE. Personal use of this material is permitted. Permission from IEEE must be obtained for all other users, including reprinting/ republishing this material for advertising or promotional purposes, creating new collective works for resale or redistribution to servers or lists, or reuse of any copyrighted components of this work in other works.

University of Bath

Alternative formats

If you require this document in an alternative format, please contact: openaccess@bath.ac.uk

Copyright and moral rights for the publications made accessible in the public portal are retained by the authors and/or other copyright owners and it is a condition of accessing publications that users recognise and abide by the legal requirements associated with these rights.

Take down policyIf you believe that this document breaches copyright please contact us providing details, and we will remove access to the work immediately and investigate your claim.

Download date: 07 Mar 2023

Water-Energy Nexus Management for Power Systems

Pengfei Zhao, Chenghong Gu, Member, IEEE, Zhidong Cao, Qian Ai, Senior Member, IEEE, Yue Xiang, Senior Member, IEEE, Tao Ding, Senior Member, IEEE, Xi Lu, Xinlei Chen and Shuangqi Li

Abstract—The water system management problem has been widely investigated. However, the interdependencies between water and energy systems are significant and the effective co-optimization is required considering strong interconnections. This paper proposes a two-stage distributionally robust operation model for integrated water-energy nexus systems including power, gas and water systems networked with energy hub systems at a distribution level considering wind uncertainty. The presence of wind power uncertainty inevitably leads to risks in the optimization model. Accordingly, a coherent risk measure, i.e., conditional value-at-risk, is combined with the optimization objective to determine risk-averse operation schemes. This two-stage mean-risk distributionally robust optimization is solved by Bender's decomposition method. Both the day-ahead and real-time operation cost are minimized with an optimal set of scheduling the multi-energy infrastructures. Case studies focus on investigating the strong interdependencies among the four interconnected energy systems. Numerical results validate the economic effectiveness of IES through optimally coordinating the multi-energy infrastructures. The proposed model can provide system operators a powerful two-stage operation scheme to minimise operation cost under water-energy nexus considering risk caused by renewable uncertainties, thus benefiting customers with lower utility bills.

Index Terms—Integrated energy system, mean-risk optimization, power-to-gas, renewable uncertainty, water-energy nexus.

NOMENCLATURE

A.	Indices and sets
t, T	Index and set of time periods.
b , B	Index and set of electricity buses.
n , N	Index and set of gas nodes.
w, W	Index and set of water nodes.
i_e , I_e	Index and set of traditional distributed generators
	(DG).
i_g , I_g	Index and set of natural gas sources.
wr, WR	Index and set of water reservoirs.

This work was supported by the National Science Fund for Distinguished Young Scholars, No. 72025404. This work was supported by the National Natural Science Foundation of China (Nos. 72042018, 71621002).

- P. Zhao and Z, Cao are with the Institute of Automation, Chinese Academy of Sciences, Beijing, China and School of Artificial Intelligence, University of Chinese Academy of Sciences, Beijing, China. (email: P. Zhao@bath.ac.uk, Zhidong.Cao@ia.ac.cn)
- P. Zhao, C.Gu (corresponding author) and S. Li are with the Department of Electronic & Electrical Engineering, University of Bath, Bath, UK.(email: P. Zhao@bath.ac.uk; C.Gu@bath.ac.uk; and S. Li@bath.ac.uk).
- Q. Ai is with the School of Electronic Information and Electrical Engineering Department of Electrical Engineering, Shanghai Jiao Tong University, Shanghai, China (e-mail: aiqian@sjtu.edu.cn).
- Y. Xiang is with College of Electrical Engineering, Sichuan University, China. (email: xiang@scu.edu.cn)
- T. Ding is with the State Key Laboratory of Electrical Insulation and Power Equipment, Department of Electrical Engineering, Xi'an Jiaotong University, Xi'an, China (e-mail: tding15@mail.xjtu.edu.cn).
- X. Lu is with the Department of Electrical Engineering, the Hong Kong Polytechnic University, Hong Kong (email: harry.lu@connect.polyu.hk)
- X. Chen is with the Electrical Engineering Department, Carnegie Mellon University, Pittsburgh, USA. (email: xinlei.chen@sv.cmu.edu)

j, J	Index and set of renewable DGs.
gt, GT	Index and set of gas turbines.
wp, WP	Index and set of water pumps.
l_e , L_e	Index and set of power lines.
l_g , L_g	Index and set of gas pipelines.
l_w , L_w	Index and set of water pipelines without pumps.
l_{wp}, L_{wp}	Index and set of water pipelines with pumps.
k_e, K_e	Index and set of power loads.
k_g , K_g	Index and set of gas loads.
k_w, K_w	Index and set of water loads.
B. Paramet	ers
$P_{k_e,t}, Q_{k_e,t}, G_{k_g,t},$	Demand of active power, reactive power, gas and
$P_{k_w,t}$	water.
$P_{m,max}$, $P_{wr,max}$	Maximum active power purchase from upper level
- m,max - wr,max	market and water purchase from reservoir.
$R_{i_e}^+, R_{i_e}^-, R_{gt}^+,$	Maximum up and down reserve capacity of
$R_{gt}^-, R_{wp}^+, R_{wp}^-$	traditional DGs, the gas turbine and water pumps.
$P_{i_e,max}, P_{i_e,min},$	Maximum and minimum limits for active power
$P_{gt,max}, P_{gt,min},$	output of traditional DGs, gas turbine output and
$P_{wp,max}, P_{wp,min},$	water pump power consumption.
$Q_{i_e,max}$,	Maximum and minimum reactive power output of
	traditional DG i_e .
$Q_{i_e,min}$	
$V_{b,max},V_{b,min}$	Maximum and minimum voltage limits.
x_{l_e}, r_{l_e}	Reactance and resistance of power line l_e .
V_0	Reference voltage magnitude.
$f_{l_e,max},qf_{l_e,max}$	Maximum active and reactive power flow of line l_e .
c_{eb}, c_{gt}	Conversion coefficient for electric boilers and the
	gas turbine.
$\omega_j^s(t)$	Forecasted output of renewable DG j at time t.
$G_{i_g,max},G_{i_g,min}$	Maximum and minimum output of gas source i_g .
$Pr_{l_g,max}$,	Maximum and minimum gas pressure of gas
$Pr_{l_g,min}$	pipeline l_g .
γ_{l_g}	Coefficient for Weymouth equation.
$f_{l_g,max}$,	Maximum gas flow of line l_g .
	Gas compressor coefficient.
CF_{l_g}	
η _e	Electrical efficiency for electrolyser.
$h_{w,max}^{l_{wp}}, h_{w,min}^{l_{wp}},$	Maximum and minimum limits for head pressure of
$h_{w,max}^{l_w}, h_{w,min}^{l_w}$	water node connected with or without water pump.
$a_{l_{wp}}, b_{l_{wp}}$	Water pump characteristic coefficients.
$R_{l_{wp}}$, $R_{l_{w}}$	Head gain and loss coefficients.
•	
π_{wp}	Water pump efficiency. Water flow for water pipeline with and without
$f_{l_{wp},max}^{s}$, $f_{l_{w},max}^{s}$	
σ. σ. σ.	pump. Water consumption efficiency for combined heat
$\sigma_{k_{cp}},\sigma_{k_{pg}},\sigma_{eb}$	and power (CHP), power-to-gas and electric boiler.
n an a	Electric and heating efficiency for CHP.
η_{cp^e} , η_{cp^e}	
η_{COP} , η_{GF}	Coefficient of performance of ground source heat
pi pi	pump (GSHP) and efficiency of gas furnace (GF). Maximum and minimum input limits of CHP,
$P_{cp,max}^{i}, P_{cp,min}^{i},$	GSHP and GF.
$P_{HP,max}^{i}$,	ODITI and OI.
$P_{HP,min}^{i}, P_{GF,max}^{i},$	
$P_{BS,max}^{ch}, P_{BS,min}^{ch},$	Maximum and minimum charging and discharging
-dch -dch	marrian fan hattami atamaa

power for battery storage.

heat for heat storage.

Maximum and minimum charging and discharging

Index and set of renewable DGs.

 $P_{BS,max}^{dch}, P_{BS,min}^{dch}$

 $P_{HS,max}^{ch}, P_{BS,min}^{ch},$

 $P_{HS,max}^{dch}, P_{HS,min}^{dch}$

IEEE TRANSACTIONS ON POWER SYSTEMS

 $\eta_{BS}^{ch}, \eta_{BS}^{dch}, \eta_{HS}^{ch},$ Charging and discharging efficiency for battery and η_{HS}^{dch} heat storage. Maximum and minimum remaining energy limits $E_{BS,max}$, $E_{BS,min}$, of battery and heat storage. $E_{HS,max}$, $E_{HS,min}$, $L_{e,t}, L_{h,t}$ Electricity and heat load of energy hub system. $\lambda_{i_e}^a, \lambda_{i_e}^b, \lambda_{i_e}^c$ Cost coefficients for generation of traditional DG λ_{i_g} Cost coefficient for output of natural gas source i_a . $\lambda_{m,\lambda_{wr}}$ Cost coefficient of power and water purchase. $\lambda_{i_{\rho}}^{+}, \lambda_{i_{\rho}}^{-}, \lambda_{GT}^{+},$ Cost coefficient for up and down reserve of traditional DGs, the gas turbine and water pumps. $\lambda_{GT}^-,\,\lambda_{wp}^+,\,\lambda_{wp}^ \lambda_m^{re}, \lambda_{i_e}^{re}, \lambda_j^{re}, \lambda_{i_a}^{re}$ Regulation cost coefficient of power purchase, traditional DGs i_e , wind turbines, natural gas sources and water reservoir. C. Variables $P_{m,t}, P_{wr,t}$ Active power and water purchase. $r_{i_e,t}^+, r_{i_e,t}^-, r_{gt,t}^+,$ Up and down reserve capacity of traditional DGs, $r_{gt,t}^-, r_{wp,t}^+, r_{wp,t}^$ the gas turbine and water pumps. Active power output of traditional DGs, gas turbine $P_{i_e,t}$, output and water pump power consumption. $P_{gt,t}, P_{wp,t}$ $Q_{i_e,t}$ Reactive power output of traditional DGs. $P_{i_{g},t}$ Output of natural gas source. $V_{b,t}^{\bar{s}}, V_{b,t}^{re}$ Scheduled and regulated voltage of bus b at time t. Active and reactive power flow and gas flow. $f_{l_e,t}, qf_{l_e,t}, f_{l_a,t}$ Injected power flow and output of electric boiler. $f_{l_e,eb,t}, P_{eb,t}$ Output of natural gas sources. $G_{i_q,t}$ $Pr_{n,t}$ Pressure of gas node n. Injected gas flow and output of gas turbine. $f_{l_g,GT,t}, P_{gt,t}$ $P_{n,t}^{P2G}$ Power consumed by the electrolyser. $G_{n,t}^{hy}$, $G_{n,t}^{hy_me}$, Gas output for overall P2G process, direct hydrogen injection, hydrogen during methanation $G_{n,t}^{hy_d}$, $G_{n,t}^{me}$ process and methanation. Required gas of carbon dioxide during methanation process.

 $h_{w,t}^{l_{wp}}, h_{w,t}^{l_{w}},$ Water pressure of pipe with and without water Elevation of water node connected with and

without pump.

 $\tilde{h}_{w,t}^{l_w}, \tilde{h}_{w,t}^{l_{wp}}$ Head loss and gain of water node. $f_{l_{wp},t},f_{l_{w},t}$ Water flow of pipe with and without water pump.

 $f_{l_e,t}^{inj}$, $f_{l_g,t}^{inj}$ Power and gas flow injection to EHSs. Power input and heat output of GSHP. $P_{COP,t}^i, P_{COP,t}^o,$ Gas input and output of gas furnace. $P_{GF,t}^i, P_{GF,t}^o$ $P_{cp,t}^{s,i}, P_{cp^e,t}^{s,o},$ Gas input and power and heat output of CHP.

 $P_{cp^h,t}^{s,o}$ $P_{BS,t}^{ch}$, $P_{BS,t}^{dch}$ $P_{HS,t}^{ch}, P_{HS,t}^{dch}$

Charging and discharging power and heat of battery and heat storage. Remaining energy of battery and heat storage.

 $E_{BS,t}$, $E_{HS,t}$ Dispatch factors of power and gas. $v_{e,t}, v_{g,t}$

I. INTRODUCTION

THE integrated energy system (IES) provides I interdependent configuration and management solution to coordinate multiple energy vectors [1]. It can be realised by the utilization of energy converters, e.g., power-to-gas (P2G), combined heat and power (CHP), heat pumps and gas turbines, etc, further intensify the operational interdependency of IES. Through optimally coordinating multiple energy infrastructures, the overall system efficiency can be significantly improved, renewable energy penetration can be highly facilitated, and environmental targets can be achieved.

Much effort has been focused on the optimization of IES, mainly achieving economic and environmental targets. A robust optimization (RO) model is proposed for an integrated powergas-heat system in smart districts [2]. This model is demonstrated on a real multi-energy district and real-world physical limitations of energy infrastructures are examined. Paper [3] develops a chance constrained operation scheme for multiple interconnected IESs in a smart city. The Cornish-Fisher algorithm effectively handles the problem. A non-convex energy hub scheduling model is proposed for an interconnected system considering battery lifetime cost in [4]. The decomposed particle swarm optimization (PSO) is utilized which outperforms the conventional PSO. Paper [5] proposes a real-time energy hub operation model considering the correlation between temperature and gas consumption. The impact of seasonal and weekly changes on operation results is extensively investigated.

2

Traditionally, water and power systems are designed and operated separately. Nevertheless, water and energy systems are mutually interdependent [6]. According to [7], 3% of U.S. electricity is facilitated by water distribution systems and approximately 80% of electricity consumed by water systems is used for distributing and pumping water. The abundant water resources largely contribute to power generation and conversion in power systems.

The existing work on joint optimization of water and power systems mainly focuses on reducing system operation cost and gas emissions. Paper [8] proposes an optimal water-power usage by controllable assets considering the couplings in an integrated water and power system (IWPS). A distributed algorithm based on the alternating direction method of multipliers helps pursue individual objectives. In [9], a coordinated day-ahead optimization model for IWPS is proposed considering the hydraulic constraints of water systems. An energy flexibility model for water systems is designed to offer the feasible energy flexibility capacity to the system operator. Paper [10] proposes an optimization model for the demand-side management of IWPS. The water system is treated as an effective resource to manage renewable generation. Stochastic programming (SP) based multistage fuzzy optimization is developed for a combined operation and planning problem in an IWPS considering uncertain power demand [11].

The enormous interdependencies among each subsystem are realized by the strong couplings for subsystems with multiple energy converters facilitated. CHP enables the conversion from gas to both heat and electricity. P2G facilities can convert excessive renewable power generation to synthetic natural gas; The conversion from gas to power is mainly realized by utilizing gas turbines; Ground source heat pump (GSHP) and gas furnace (GF) enable the heat conversion from power and gas respectively; The electrolyses in the P2G facilities consume the water from water system; The energy conversion from CHP relies on the water supply; Water pumps consume electricity from power system; The electricity boiler in the water system requests the electricity supply to convert the water to heat. Modelling and optimizing all the subsystems as an entity can facilitate the economy and security of the entire system.

The inherent interdependencies between subsystems in IES have been promoted due to increasing energy demand growth. lower prices of gas resources, and emerging conversion technologies for interconnecting subsystems [12-14]. The aforementioned literature in the IES demonstrates the benefits of interdependencies [1-7, 14-16]. Moreover, the integration of

3

multiple energy systems and water systems will further strengthen the couplings and interdependencies.

In the existing literature, the uncertainty pertaining to renewable generation in IES operation is commonly handled by SP [15, 16] and RO [2]. SP assumes that the distribution of uncertain variables is known. However, obtaining explicit distributions is impractical and the scenario approach will lead to computational burden in optimization. RO copes with uncertainty considering all realizations, including the worst-case renewable fluctuation scenario, which ensures system robustness but sacrifices system cost effectiveness. Distributionally robust optimization (DRO), which employs partial distributional information to capture the ambiguous uncertainty distributions, can overcome the limitations and deficiencies of SP and RO [17]. Recently, DRO has been applied in the operation of distribution systems. Paper [18] proposes distributionally robust scheduling for integrated electricity and gas systems considering demand response. The revenue from demand response is maximized and expected load shedding cost is minimized. A distributionally robust operation for electric vehicle aggregators is proposed in [19]. The DRO technique is effective for avoiding unnecessary costs considering temporal and spatial characteristics of the charging demands of aggregators.

DRO employs ambiguity sets to capture the uncertainties pertaining to known distributional information. The optimization results will be intractable or over-conservative if the ambiguity set is not chosen appropriately [20]. There are two common methods to characterize ambiguity sets, moment-based ambiguity set and discrepancy-based ambiguity set. The former one has simple tractable reformulations, e.g., semidefinite program (SDP) or second-order cone program (SOCP). Nevertheless, different distributions might have the same moment information, which introduces challenges for determining the worst-case distribution. Discrepancy-based ambiguity set measures the statistical distance between the reference distribution and candidate distributions. Kullback-Leibler (KL) divergence is widely applied in operation problems in the area of power systems [21, 22].

The uncertainties bring risks into economic operation. Intuitively, risks in the proposed IES operation model can lead to abnormal high operation cost. Mean-risk optimization considers a coherent trade-off between system economic performance and risk, which has been applied with SP on energy system operation [23-25]. Paper [23] develops a mean-risk stochastic programming model for unit commitment considering renewable energy uncertainty. A conditional value-at-risk (CVaR) is incorporated to assess the risk from renewable energy uncertainty. In [25], a day-ahead operational planning model for a regional energy service provider with electricity price uncertainty is proposed. The CVaR criterion is employed to hedge against the uncertainty.

This paper aims at constructing a two-stage mean-risk DRO model, which is helpful for providing system operators the trade-off operation scheme between operation cost and risk mitigation. Based on the common IES, this paper proposes a coordinated optimization for integrated water-energy nexus system (IWENS) with the connection of multiple energy hub systems (EHSs) containing power, gas and water systems. This paper proposes a two-stage mean-risk distributionally robust optimization (TSMR-DRO) for IWENS considering the uncertainty of wind power generation. The two-stage model includes day-ahead and real-time operation schemes, prior to and after wind uncertainty realization. The ambiguity set for capturing wind uncertainty is

constructed using KL divergence. The coherent risk measure, i.e., CVaR is employed to model the trade-off between expected computational performance and risk. Bender's decomposition is applied to solve the problem in an iterative manner. The proposed IWENS provides utility system operators a two-stage operation scheme to minimize operation cost when dealing with enormous cross energy vector interdependencies.

The main contributions of this paper are as follows:

- 1) It develops an innovative IWENS structure networked with EHSs and renewable distributed generators (DGs) for integrated energy distribution systems. The intricate nexus between power, gas and water is extensively modelled.
- 2) It aggregates considerable interconnections and converters among subsystems, e.g., gas turbines, P2G facilities, CHP, GF, GSHP, water pumps and electric boilers. The enormous interdependencies and interactions between energy sectors are beneficial for improving economic efficiency and sustainability.
- 3) A two-stage DRO model is applied to optimize both dayahead and real-time operation schemes. The day-ahead stage determines the initial operation scheme with reserve capacity from traditional DGs and CHPs and water pumps.
- 4) It combines DRO with mean-risk optimization. The benefits of the proposed DR-MRO is in threefold: i) it overcomes the shortages of SO and RO by using partial distributional information with moderate robustness, ii) the KL divergence-based ambiguity set can flexibly shape the considered candidate distributions compared with moment-based ambiguity sets and accordingly yields less-conservative results and iii) the trade-off between economic performance and risk can be realized based on the incorporation of CVaR on the objective function.

The remainder of this paper is organized as follows. Section II presents the objective function and constraints for both day-ahead and real-time stages. Section III proposes the method for solving KL divergence-based TSMR-DRO considering the incorporation of CVaR. The case studies for demonstrating the advantages of IWENS and TSMR-DRO are given in Section IV. Finally, section V concludes the entire paper.

II. PROBLEM FORMULATION

This section proposes the mathematical modelling for IWENS including both day-ahead and real-time operation schemes. Then the risk measure is given. Finally, the objective function is illustrated. The assumption is made that the entire IWENS is owned by a single entity which controls all the energy infrastructures and there is no trading between each subsystem.

The proposed IWENS structure is given in Fig. 1, where the power, gas and water systems are shown in black, navy and blue. The power and gas systems have three interconnection points: i) buses 6 and 15 in power system are connected with node 2 and 6 in the gas system via gas turbines and P2G facility at bus 10 is connected with gas node 3. The two EHSs are sourced from both power and gas systems. The water distribution system interconnects with all the other subsystems: i) water node 11 is connected with the P2G facility for the water electrolysis process, ii) water node 2 connects with EHSs 1 and 2 for CHP conversion; iii) water pump at nodes 1, 2 and 6 consume electricity from EHS 1 and iv) water system is connected with EHS via an electric boiler. The IWENS contains two EHSs. Each EHS contains a CHP, a GSHP, a GF. EHS 1 contains an energy storage system

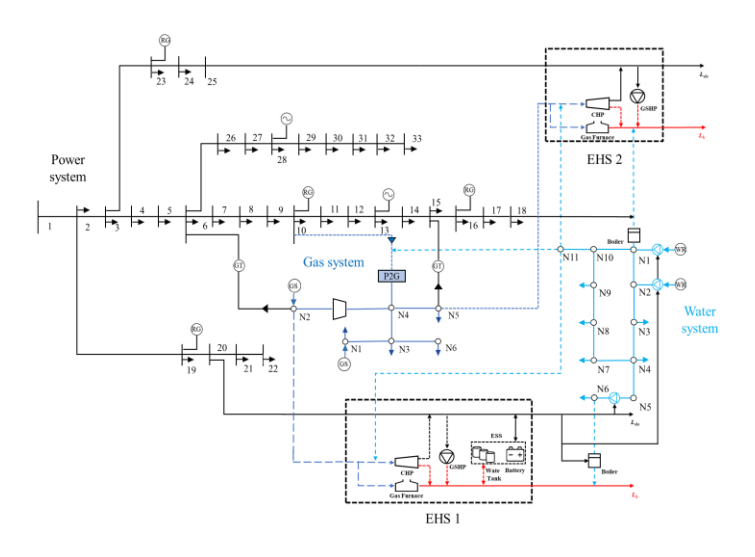


Fig. 1. Proposed structure of IWENS.

(ESS). The ESS is composed of a battery storage and a water tank for storing excessive electricity and heating respectively [26, 27].

A. Day-ahead Operation

The day-ahead optimization schedules power generation plan of traditional DGs and the reserve capacity dispatch from traditional DGs, gas turbines and water pumps considering the operation status of other energy infrastructures. The constraints are in (1)-(40). The power purchase from upper-level market is given in (1). The reserve capacity from traditional DGs, gas turbines and water pumps are shown in (2) and (3), followed by their output limits in (4) and (5). Constraint (6) limits the reactive power output of traditional DGs. Constraints (8) and (9) are the linearised DistFlow equations for distribution networks. They are obtained based on the assumption that i) losses are negligible, ii) the voltage at each bus is close to 1.0 p.u. and iii) the voltage at the reference bus is 1.0 p.u. [28-30]. Constraint (10) is the output of electric boiler. The balancing conditions for active and reactive power are in (11) and (12).

The output of the natural gas source is constrained in (13). Constraints (14) and (15) are used to limit the gas pressure. Note that the gas pressures of initial nodes are always higher than terminal nodes due to the unidirectional gas flow. Accordingly, constraint (15) is used to ensure unidirectional gas flow. Equation (16) is the Weymouth gas flow equation that characterizes the relationship between gas pressure and flow. The gas flow of gas pipelines is constrained in (17). The output of gas turbine is in (18). Equation (19) presents the relationship between the gas pressure of initial and terminal nodes of gas compressors. The excessive renewable generation can be converted into gas via P2G. The electrolyser splits water into hydrogen and oxygen. The output of electrolyser is given in (20). The nodal gas balance is given in (21).

In water distribution systems, constraint (22) limits the output of reservoir. Equation (23) is the constraint of water pressure limit for pipes installed with and without water pumps. In (24)-(27). the hydraulic characteristics of water pipes are given for pipes installed with and without water pump in terms of head gain and loss. The pressure head gain of water pump is in (26). Equation (27) describes the hydraulic characteristic of pipes without pumps using Darcy-Weisbach equation [31]. The power consumption of

water pump is in (28). Constraint (29) limits the water flow magnitude. The mass balance for the water system is in (30). The water consumption of energy converters is also given in (30), where $\sigma_{k_{cp}}P_{cp,t}^{s,i}$, $\sigma_{k_{pg}}P_{n,t}^{s,P2G}$, and $\sigma_{eb}P_{eb,t}^{s}$ represent the water consumed from CHPs, P2Gs and electric boilers, respectively [32, 33].

In EHSs, the energy conversion of CHP, GF and GSHP are in (31)-(33). The input limit for all converters is given in (34). Equation (35) is the constraint of the charging and discharging power and heat for ESSs. Constraint (36) and (37) limit the remaining energy for battery storage and water tank. Constraint (38) presents the coupling relationship for the EHSs, which is the energy balance constraint of EHSs.

$$0 \le P_{m,t}^s \le P_{m,max} \tag{1}$$

$$0 \le r_{\{\cdot\},t}^+ \le R_{\{\cdot\}}^+, \{\cdot\} = i_e, gt, wp$$
 (2)

$$0 \le r_{\{\cdot\},t}^- \le R_{\{\cdot\}}^-, \{\cdot\} = i_e, gt, wp \tag{3}$$

$$P_{\{\cdot\},t}^{s} + r_{\{\cdot\},t}^{+} \le P_{\{\cdot\},max}, \{\cdot\} = i_e, gt, wp$$
 (4)

$$P_{\{\cdot\},min} \le P^{s}_{\{\cdot\},t} - r^{-}_{\{\cdot\},t}, \{\cdot\} = i_e, gt, wp \tag{5}$$

$$Q_{i_{\varrho},min} \le Q_{i_{\varrho},t}^s \le Q_{i_{\varrho},max} \tag{6}$$

$$V_{b,min} \le V_{b,t}^s \le V_{b,max} \tag{7}$$

$$V_{b,min} \leq V_{b,t}^{s} \leq V_{b,max}$$

$$V_{b}^{s,ini} - V_{b}^{s,ter} = (f_{le,t}^{s} r_{le} + q f_{le,t}^{s} x_{le}) / V_{0}$$

$$0 \leq \{\cdot\}_{le,t}^{s} \leq \{\cdot\}_{le,max}^{s}, \{\cdot\} = f, qf$$

$$(7)$$

$$(8)$$

$$0 \le \{\cdot\}_{l=t}^{s} \le \{\cdot\}_{l=max}^{s}, \{\cdot\} = f, qf \tag{9}$$

$$P_{eb,t}^{s} = c_{eb} f_{le,eb}^{s} \tag{10}$$

$$0 \leq \{\cdot\}_{l_{e},t}^{S} \leq \{\cdot\}_{l_{e},max}^{S}, \{\cdot\} = f, qf$$

$$P_{eb,t}^{S} = c_{eb}f_{l_{e},eb}^{S}$$

$$\sum_{l_{e}\in l_{e}} P_{l_{e},t}^{S} + \sum_{j_{e}} \omega_{j,t}^{S} + \sum_{l_{e}\in L_{e}} f_{l_{e},t}^{s,ini} - \sum_{l_{e}\in L_{e}} f_{l_{e},t}^{s,er} + P_{gt,t}^{S} = \sum_{k_{e}\in K_{e}} P_{k_{e},t} + \sum_{l_{e}\in L_{e}} f_{l_{e},t}^{s,inj}$$

$$+ \sum_{eb\in EB} P_{eb,t}^{S} + \sum_{n\in N} P_{n,t}^{S,PSG} + \sum_{wp\in Wp} P_{wp,t}^{S}$$

$$\sum_{l_{e}\in l_{e}} Q_{l_{e},t}^{S} + \sum_{l_{e}\in L_{e}} qf_{l_{e},t}^{s,ini} - \sum_{l_{e}\in L_{e}} qf_{l_{e},t}^{s,ter} = \sum_{k_{e}\in K_{e}} Q_{k_{e},t}$$

$$(12)$$

$$\sum_{l_{s} \in I_{o}} Q_{l_{e},t}^{s} + \sum_{l_{s} \in I_{o}} q_{l_{e},t}^{s,ini} - \sum_{l_{s} \in I_{o}} q_{l_{e},t}^{s,ter} = \sum_{k_{s} \in K_{o}}^{wp \in WP} Q_{k_{e},t}$$
 (12)

$$G_{i_g,min} \le G_{i_g,t}^s \le G_{i_g,max} \tag{13}$$

$$Pr_{l_{a},min}^{2} \le Pr_{l_{a},t}^{s^{2}} \le Pr_{l_{a},max}^{2}$$
 (14)

$$Pr_{l-t}^{s,ini} \ge Pr_{l-t}^{s,ter} \tag{15}$$

$$Pr_{l_{g,min}}^{s} \leq Pr_{l_{g,t}}^{s^{2}} \leq Pr_{l_{g,max}}^{s,ter}$$

$$Pr_{l_{g,t}}^{s,int} \geq Pr_{l_{g,t}}^{s,ter}$$

$$f_{l_{g,t}}^{s} = \gamma_{l_{g}} \left(Pr_{l_{g,t}}^{s,int^{2}} - Pr_{l_{g,t}}^{s,ter^{2}} \right)$$
(16)

$$0 \le f_{l_a,t}^s \le f_{l_a,max}^s$$
(17)

$$P_{gt,t}^s = c_{GT} f_{l_g,gt,t}^s \tag{18}$$

$$Pr_{l_a,t}^{ter} \le CF_{l_a}Pr_{l_a,t}^{ini} \tag{19}$$

$$T_{lg,t} \leq CF_{lg}PT_{lg,t} \tag{19}$$

$$p_{s,P2G} \tag{20}$$

$$G_{n,t}^{s,hy} = \eta_e \frac{P_{n,t}^{s,P2G}}{\Omega_{hy}}$$
 (20)

$$\sum_{l_g \in I_g} G_{l_g,t}^s + \sum_{n \in N} G_{n,t}^{s,hy} + \sum_{l_g \in L_g} f_{l_g,t}^{s,ini} - \sum_{l_g \in L_g} f_{l_g,t}^{s,ter}$$

$$= \sum_{k_g \in K_g} G_{k_g,t} + \sum_{l_g \in L_g} f_{l_g,g,t,t}^{s} + \sum_{l_g \in L_g} f_{l_g,t}^{s,inj}$$
(21)

$$0 \le P_{wr,t}^s \le P_{wr,max} \tag{22}$$

$$h_{w,min}^{\{\cdot\}} \le h_{w,t}^{s,\{\cdot\}} \le h_{w,max}^{\{\cdot\}}, \{\cdot\} = l_w, l_{wn}$$
 (23)

$$0 \leq P_{wr,t}^{s} \leq P_{wr,max}$$

$$h_{w,min}^{\{\cdot\}} \leq h_{w,t}^{\{\cdot\}} \leq h_{w,max}^{\{\cdot\}}, \{\cdot\} = l_{w}, l_{wp}$$

$$\tilde{h}_{\{\cdot\},t}^{s} = \left(h_{w,t}^{s,\{\cdot\},int} + \bar{h}_{w,t}^{s,\{\cdot\},int}\right) - \left(h_{w,t}^{s,\{\cdot\},ter} + \bar{h}_{w,t}^{s,\{\cdot\},ter}\right), \{\cdot\} = l_{w}, l_{wp}$$

$$(24)$$

$$\tilde{h}_{l_{wn},t}^s \ge 0 \tag{25}$$

$$\tilde{h}_{l_{wp,t}}^{s} + a_{l_{wp}} f_{l_{wp,t}}^{s} + b_{l_{wp}} = R_{l_{wp}} f_{l_{wp,t}}^{s}^{2}$$

$$\tilde{h}_{l_{w,t}}^{s} = R_{l_{w}} f_{l_{wp,t}}^{s}^{2}$$
(26)

$$\tilde{h}_{lw,t}^s = R_{lw} f_{lwn,t}^{\ s}^{\ 2} \tag{27}$$

$$P_{wp,t}^{s} = \left(a_{l_{wp}} f_{l_{wp},t}^{s}^{2} + b_{l_{wp}} f_{l_{wp},t}^{s}\right) / \pi_{wp}$$
 (28)

$$0 \le f_{\{i\}_t}^s \le f_{\{i\}_{max'}}^s \{\cdot\} = l_{w'} l_{wn} \tag{29}$$

$$P_{wp,t}^{s} = \left(u_{lwp}I_{lwp,t} + bI_{lwp}I_{lwp,t}\right)/n_{wp}$$

$$0 \le f_{\{\},t}^{s} \le f_{\{\},max}^{s} \{\cdot\} = I_{w}, I_{wp}$$

$$\sum_{wr \in WR} P_{wr,t}^{s} + \sum_{\{\cdot\} \in L_{w}, L_{wp}} f_{\{\cdot\},t}^{s,int} - \sum_{\{\cdot\} \in L_{w}, L_{wp}} f_{\{\cdot\},t}^{s,ter}$$

$$= \sum_{k_{pg} \in K_{pg}} \sigma_{k_{pg}} P_{n,t}^{s,p2G} + \sum_{k_{cp} \in K_{cp}} \sigma_{k_{cp}} P_{cp,t}^{s,i} + \sum_{eb \in EB} \sigma_{eb} P_{eb,t}^{s} + \sum_{k_{w} \in K_{w}} P_{k_{w},t}$$

$$P_{\{\cdot\},t}^{s,o} = \eta_{\{\cdot\}} P_{\{\cdot\},t}^{s,i}, \{\cdot\} = COP, GF$$

$$(31)$$

$$P_{G,t}^{s,o} = \eta_{G} P_{G,t}^{s,i} \{\cdot\} = COP_{t} GF \tag{31}$$

$$P_{cp^e,t}^{s,o} = \eta_{cp^e} P_{cp,t}^{s,i} \tag{32}$$

$$P_{cp^h,t}^{s,o} = \eta_{cp^h} P_{cp,t}^{s,i} \tag{33}$$

$$P_{\{\},min}^{i} \le P_{\{\},t}^{i} \le P_{\{\},max}^{i}, \{\cdot\} = cp, COP, GF$$
(34)

IEEE TRANSACTIONS ON POWER SYSTEMS

$$P_{\{\cdot\},min}^{s,ch/dch} \le P_{\{\cdot\},t}^{s,ch/dch} \le P_{\{\cdot\},max}^{s,ch/dch}, \{\cdot\} = BS, HS$$

$$(35)$$

$$E_{\{\cdot\},t}^{s} = E_{\{\cdot\},t-1}^{s} + \sum_{1}^{t} P_{\{\cdot\},t}^{s,ch} \eta_{\{\cdot\}}^{ch} - P_{\{\cdot\},t}^{s,dch} / \eta_{\{\cdot\}}^{dch}, \{\cdot\} = BS, HS$$
 (36)

$$E_{\{\cdot\},min} \le \bar{E}_{\{\cdot\},t}^S \le E_{\{\cdot\},max}, \{\cdot\} = BS, HS$$

$$[L_{++} + P_{S_0}^S]$$
(37)

$$E_{\{\cdot\},min} \leq E_{\{\cdot\},max}^{s}, \{\cdot\} = BS, HS$$

$$\begin{bmatrix} L_{e,t} + P_{BS,t}^{s} \\ L_{h,t} + P_{HS,t}^{s} \end{bmatrix} = \begin{bmatrix} 1 - v_{e,t}^{s} & v_{g,t}^{s} \eta_{CHP^{e}} (1 - v_{e,t}^{s}) \\ v_{e,t}^{s} \eta_{COP} & v_{g,t}^{s} (\eta_{CHP^{h}} + \eta_{CHP^{e}} v_{e,t}^{s} \eta_{COP} + \eta_{GF} - v_{g,t}^{s} \eta_{GF}) \end{bmatrix} \times \begin{bmatrix} f_{l_{e},t}^{s,inj} \\ f_{l_{g},t}^{s,inj} \end{bmatrix}$$
(38)

B. Real-time Operation

In the second stage, corrective operation schemes are deployed based on the realization of wind uncertainty. Equation (39) is the constraint for the regulated power output of traditional DGs and gas turbine. And (40) is the new power balance constraint considering wind uncertainty. Due to space limitation, the constraints for real-time operation are not listed. Apart from (39) and (40), the rest second-stage constraints are the same as the first-stage constraints, where the superscript 's' on each variable is changed to 're'. 's' represents the scheduled decision variables in the first stage and 're' represents the regulated decision variables in the second stage. The regulated decision variables are summarized in (41).

$$P_{\{:\},t}^{s} - r_{\{:\},t}^{-} \leq P_{\{:\},t}^{re} \leq P_{\{:\},t}^{s} + r_{\{:\},t}^{+}, \{\cdot\} = i_{e}, gt, wp$$

$$\sum_{l_{e} \in l_{e}} P_{l_{e},t}^{re} + \sum_{j \in J} \xi_{j,t} + \sum_{l_{e} \in L_{e}} f_{l_{e},t}^{re,ini} - \sum_{l_{e} \in l_{e}} f_{l_{e},t}^{re,ire} + P_{GT,t}^{re} = \sum_{k_{e} \in K_{e}} P_{k_{e},t} + \sum_{l_{e} \in L_{e}} f_{l_{e},t}^{re,inj}$$

$$+ \sum_{eb \in BB} P_{eb,t}^{re} + \sum_{n \in N} P_{n,t}^{re,P2G} + \sum_{wp \in WP} P_{wp,t}^{re,P2G}$$

$$(40)$$

$$y = \begin{cases} P_{m,t}^{re}, P_{i_e,t}^{re}, P_{g_{t,t}}^{re}, Q_{i_{e,t}}^{re}, V_{b,t}^{re}, f_{l_e,t}^{re}, q_{l_{e,t}}^{re}, P_{l_{g_t}}^{re}, P_{l_{g_t}}^{re}, f_{l_g,t}^{re}, P_{g_{t,t}}^{re}, P_{g_{t,t}}^{re}, P_{g_{t,t}}^{re}, P_{l_{e,t}}^{re}, P_{l_{e,t}}^{re},$$

C. Objective function

In the first stage, the day-ahead objective in (42) is to minimize total operation cost, including i) generation cost of traditional DGs and natural gas sources, ii) power purchase cost from dayahead upper-level market, iii) water purchase cost from water reservoirs, iv) cost for reserve capacity from traditional DGs, gas turbines and water pumps.

bines and water pumps.
$$\Gamma_{1} = \min \sum_{\substack{i_{e} \in I_{e}, i_{g} \in I_{g}, t \in T, wr \in WR, gt \in GT \\ + \lambda_{wr} P_{wr,t}^{S} + \lambda_{i_{g}} P_{i_{g},t}^{S} + \lambda_{i_{e}}^{+} P_{i_{e},t}^{+} + \lambda_{i_{e}}^{c} P_{i_{e},t}^{S} + \lambda_{i_{e}}^{C} \\
= i_{o}, at., wp$$
(42)

The second-stage problem considers real-time redispatch and corrective actions pertaining to wind uncertainty. The objective function contains the penalties due to the overestimation or underestimation of scheduling in the first stage. The first-stage generation decisions include the scheduled power and water purchase, wind generation forecast, scheduled output of traditional DGs and natural gas sources. The minimization of deviation between scheduled and regulated results promotes the utilization of renewable energy [34].

$$\Gamma_{2} = \min \sum_{\substack{i_{e} \in I_{e}, i_{g} \in I_{g}, t \in T, wr \in WR}} \lambda_{m}^{re} | P_{m,t}^{s} - P_{m,t}^{re}| + \lambda_{j}^{re} | \omega_{j,t}^{s} - \xi_{j,t}|$$

$$+ \lambda_{i_{e}}^{re} | P_{i_{e},t}^{s} - P_{i_{e},t}^{re}| + \lambda_{i_{g}}^{re} | P_{i_{g},t}^{s} - P_{i_{g},t}^{re}|$$

$$+ \lambda_{i_{e}}^{re} | P_{s_{e},t}^{s} - P_{i_{e},t}^{re}|$$

$$+ \lambda_{i_{e}}^{re} | P_{s_{e},t}^{s} - P_{i_{g},t}^{re}|$$

$$(43)$$

III. METHODOLOGY

The proposed DR-IWENS is a two-stage minmax DRO model, which can be solved by the Bender's decomposition, shown in this section. Firstly, the linear problem is represented by a compact form for notation brevity. Secondly, the KL divergence-

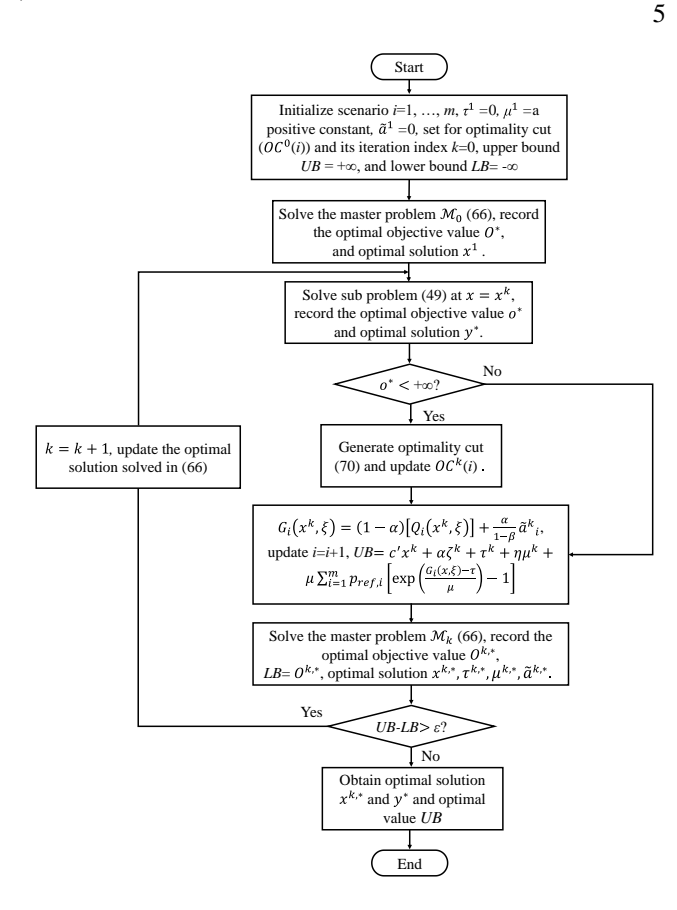


Fig. 2. Flowchart of Bender's decomposition approach.

based ambiguity set is used to define the uncertainty. Then, CVaR is derived. The final step incorporates the mathematical reformulation and decomposition methods for solving the problem.

A. Formulation in Brevity

The original problem can be represented by vectors and matrices to represent the objective function and constraints for notation simplicity. Compared to the proposed risk-averse model, the traditional risk-neutral DRO model does not consider risk factor, which is given in (44).

$$\min_{x \in X} c'x + \sup_{p \in D_{\xi}} E_p[Q(x,\xi)] \tag{44}$$

Based on the traditional risk-neutral DRO model, the risk measure can be included in the second stage problem, shown below:

$$\min_{x \in X} c'x + \sup_{p \in D_{\xi}} \left\{ (1 - \alpha) E_p[Q(x, \xi)] + \alpha R(Q(x, \xi)) \right\}$$
 (45)

$$\begin{aligned}
& p \in D_{\xi} \\
\text{s.t. } Ax \le b, \\
& Q(x, \xi) = \min_{y} f'y
\end{aligned} \tag{46}$$

$$Q(x,\xi) = \min_{y} f'y \tag{47}$$

s.t.
$$Ex + Fy + G\xi \le h$$
, (48)

The risk-averse objective function (45) is to minimize the sum of the first-stage objective c'x, the weighted expected secondstage objective $(1 - \alpha)E_p[Q(x, \xi)]$, and the weighted risk measure $\alpha R(Q(x,\xi))$. D_{ξ} denotes the ambiguity set, containing distribution p. The weighting factor α ranges between 0 and 1. When $\alpha=0$, (45) degrades to the traditional risk-neutral DRO. Equation (46) presents the first-stage constraints. The recourse process is represented by (47) and (48), where f denotes the coefficient of (47).

B. KL Divergence-Based Ambiguity Set

The discrepancy-based ambiguity set is constructed based on measuring the distance between probability distributions, i.e., the divergence tolerance η in (49). The true and reference probability distribution are represented by p and p_{ref} , respectively. The KL divergence between p and p_{ref} is defined in (50), where $p\left(\xi\right)$ and $p_{ref}(\xi)$ are the probability density functions.

$$Dis = \{ p \in D_{\xi_i} | D_{\xi_i}(p || p_{ref}) \le \eta \}$$
 (49)

$$D_{\xi,}(p||p_{ref}) = \int f(\xi) \log \frac{p(\xi)}{p_{ref}(\xi)} d\xi$$
(50)

KL-divergence function of variable a is in (51) and it will be used in the dual formulation to solve the inner maximization problem in section D.

$$\varphi_{KL}(a) := a \log a - a + 1 \tag{51}$$

C. Coherent Risk Measure

The probability of the second-stage objective function $Q(x,\xi)$, i.e., the corrective operation cost including load shedding lost, is restricted by the threshold ζ . As an emerging risk measure method, CVaR is a coherent risk measure, which is convex, transition-equivalent, and monotonic. The original expression of CVaR is in (52), which can be further approximated by (53) to avoid the computation of multiple integral [35]. $[Q(x,\xi) - \zeta]^+$ represent determining the larger value between $Q(x,\xi) - \zeta$ and

$$CVaR_{\beta}(Q(x,\xi)) := \frac{1}{1-\beta} \int_{Q(x,\xi) \ge VaR_{\beta}(x,\xi)} Q(x,\xi) p(\xi) d\xi$$
 (52)

$$CVaR_{\beta}(Q(x,\xi)) := \min_{\zeta \in \mathbb{R}} \left\{ \zeta + \frac{1}{1-\beta} E_p[Q(x,\xi) - \zeta]^+ \right\}$$
 (53)

D. Risk-Averse DRO

The proposed TSMR-DRO is formulated as (54) with weighted CVaR. Equation (55) can be derived by substituting CVaR in (56) with (55).

$$\min_{x \in X} c'x + \sup_{p \in D_{\xi}, \xi = \Delta P_k, \xi_j} \left\{ (1 - \alpha) E_p[Q(x, \xi)] + \alpha C V a R_{\beta}(Q(x, \xi)) \right\}$$
 (54)

$$\min_{x \in X} \left\{ c'x + \sup_{p \in D_{\xi}, \xi = \Delta P_{k}, \xi_{j}} \min_{\zeta \in \mathbb{R}} \left\{ \alpha \zeta + E_{p}[G(x, \xi)] \right\} \right\}
G(x, \xi) := (1 - \alpha)[Q(x, \xi)] + \frac{\alpha}{1 - \beta} \tilde{\alpha}
\text{s.t.} Q(x, \xi) - \tilde{\alpha} - \zeta \le 0, \tilde{\alpha} \ge 0$$
(55)

Based on the proof in [36] on the strong duality, (55) can be reformulated into (56) and then (57).

$$\min_{x \in X} \left\{ c'x + \min_{\zeta \in \mathbb{R}} \sup_{p \in D_{\xi}, \xi = \Delta P_k, \xi_j} \left\{ \alpha \zeta + E_p[G(x, \xi)] \right\} \right\}$$
(56)

$$\min_{x \in X} \left\{ c'x + \alpha \zeta + \max_{p \in D_{\xi, \xi} = \Delta P_k, \xi_j} \left\{ \sum_{i=1}^m p_i G_i(x, \xi) \right\} \right\}$$
(57)

The inner maximization problem can be handled by the Lagrange function (58) with its dual formulation (64).

$$\mathcal{L}(p,\tau,\mu) = \sum_{i=1}^{m} p_{i}G_{i}(x,\xi) + \tau \left(1 - \sum_{i=1}^{m} p_{i}\right) + \mu \left(\eta - \sum_{i=1}^{m} p_{ref,i} \varphi_{KL} \left(\frac{p_{i}}{p_{ref,i}}\right)\right)$$
(58)

$$\max \mathcal{L}(p, \tau, \mu) = \tau + \eta \mu + \mu \sum_{i=1}^{m} p_{ref, i} \left[\exp \left(\frac{G_i(x, \xi) - \tau}{\mu} \right) - 1 \right]$$
 (59)

According to Slater's condition [37], when η is larger than 0, the below reformulation can be made:

$$\max_{p \in D_{\xi}, \xi = \Delta P_k, \xi_j} \left\{ \sum_{i=1}^m p_i G_i(x, \xi) \right\} = \min_{\tau, \mu \ge 0} \max \mathcal{L}(p, \tau, \mu)$$
(60)

$$= \min_{\tau, \mu \ge 0} \left\{ \tau + \eta \mu + \mu \sum_{i=1}^{m} p_{ref, i} \left[\exp \left(\frac{G_i(x, \xi) - \tau}{\mu} \right) - 1 \right] \right\}$$
 (61)

Substituting the inner maximization in (57) with (61), the below derivation can be obtained.

$$\begin{split} \min_{\zeta,\tau,\mu\geq 0} \left\{ c'x + \alpha\zeta + \tau + \eta\mu + \mu \sum_{i=1}^{m} p_{ref,i} \left[\exp\left(\frac{G_i(x,\xi) - \tau}{\mu}\right) - 1 \right] \right\} \\ \text{s.t. } x \in X, \, Q(x,\xi) - \tilde{\alpha} - \zeta \leq 0, \, \tilde{\alpha} \geq 0, \\ G(x,\xi) := (1-\alpha) [Q(x,\xi)] + \frac{\alpha}{1-\beta} \tilde{\alpha} \end{split} \tag{62}$$

However, the optimization problem (62) is nonlinear, which needs to be linearized before decomposition. For a given $x = x^k$, when $Q(x^k, \xi) < \infty$, then $Q(x^k, \xi)$ is subdifferentiable [38] and equation (63) can be obtained, where $Dual(x^k) = argmax\{\pi'(h - Ex^k): F'\pi \le f\}$ is the set of optimal solutions of dual problem for (47) and $\pi^{k,i} \in$ $Dual(x^k)$ is optimal solution for the *i*th and *k*th iterations.

$$\partial Q(x^k, \xi) = -E'Dual(x^k) \tag{63}$$

Let $s^k := \frac{G_i(x^k,\xi) - \tau^k}{\mu^k}$ and $F_i^k := \mu^k [\exp(s^k) - 1]$, the subgradient of F_i^k can be described as: $\partial F_i^k = \left[(1 - \alpha) \exp(s^k) E' \pi^{k,i}, (1 - s^k) \exp(s^k) - 1, -\exp(s^k), \frac{\alpha}{1 - \beta} \exp(s^k) \right] \tag{64}$

$$\partial F_i^k = \left[(1 - \alpha) \exp(s^k) E' \pi^{k,i}, (1 - s^k) \exp(s^k) - 1, -\exp(s^k), \frac{\alpha}{1 - \beta} \exp(s^k) \right]$$
 (64)

Based on the subgradient inequality of convex function, the below equation can be obtained. The optimality cut can be defined in (66).

$$F_i(x,\mu,\tau,\tilde{a}_i) \ge F_i(x^k,\mu^k,\tau^k,\tilde{a}_i^k) + \partial F_i^{k-1}(x-x^k,\mu-\mu^k,\tau-\tau^k,\tilde{a}_i-\tilde{a}_i^k)$$

$$\tag{65}$$

$$F_{i}(x,\mu,\tau,\tilde{\alpha}_{i}) \geq \left[G_{i}(x^{k},\xi) + (1-\alpha)(\pi^{k,i})'Ex^{k} - \frac{\alpha\tilde{\alpha}_{i}^{k}}{1-\beta}\right] + \partial F_{i}^{k}(x,\mu,\tau,\tilde{\alpha}_{i})$$

$$\tag{66}$$

A Bender's decomposition is employed to solve the TSMR-DRO problem and the flowchart is given in Fig. 2.

IV. CASE STUDIES

The proposed DR-IWENS is verified on a district water-energy nexus system consisting of a modified IEEE 33-bus system, a 6node gas system, two EHSs and a 11-node water system, where generator information is given in TABLEs I, II and III. The power system has two traditional DGs and four renewable DGs. The power system is connected with the gas system via two gas turbines and a P2G facility. Two EHSs are supplied by both electricity buses 20 and 25 and natural gas nodes 2 and 5. The technical parameters of EHSs can be found in the existing publications [3, 39]. The water consumption of P2G and CHPs are supplied by node 11 of the water system. Electric boilers enable the heating conversion from power and water. This study considers 5 cases for demonstrating the effectiveness of the model, which is presented in TABLE IV.

The economic performance for all the cases is studied firstly in this section, followed by the optimal schedule of interdependent energy converters. The mathematical performance with different risk-aversion parameters is given in section C.

A. Economic Performance of Each Subsystem

The economic performance for all the cases is given in TABLE V, which incorporates the operation cost of power system, gas system, water system and entire IES. Overall, case 3 with twice output of the renewable DGs yields the lowest total operation cost whilst the total operation cost of case 5 is the highest when gas price is twice of case 1. Case 2 is the risk-neutral optimization without considering CVaR in the objective function. It can be seen that the operation cost of each subsystem is lower than those of case 1. The total operation cost, i.e., \$36687, is 91% of that of case 1. When the output of renewable DGs is doubled in case 3, the most distinct feature is the operation cost of power system, which is only \$13275. Meanwhile, the gas system operation cost is also reduced by \$3468 since there is more excessive renewable output injecting to the gas system via the P2G facility. However, the water system operation cost is \$348 more than that of case 1. The reason is that P2G and CHPs

TABLE I PARAMETERS OF WATER RESERVOIRS

Node No.	P _{wr,max} (m ³ /h)	λ _{wr} (\$/m³)	Elevation (m)
1	325	6.4	-252.5
2	700	2.6	-255

TABLE II PARAMETERS OF NATURAL GAS SOURCES

Node No.	P _{ig,min} (kcf/h)	P _{ig,max} (kcf/h)	λ_{i_g} (\$/kcf)
1	0	35.31	2.2
2	0	70.63	2

TABLE III GENERATOR PARAMETERS

Bus No.	$P_{i_e,max}$ (MW)	$P_{i_e,min}$ (MW)	R_i^+, R_i^- (MW)	a _i (\$/MW ²)	<i>b_i</i> (\$/MW)	<i>c_i</i> (\$)
13	1.2	0.3	0.2	6000	7100	6200
28	1.0	0.1	0.2	4500	10500	4000

TABLE IV CASE ILLUSTRATION

Case No.	Risk measure	Renewable DG capacity	P2G connection	Gas generation price
1	Yes	Nominal	Yes	Nominal
2	No	Nominal	Yes	Nominal
3	Yes	Twice	Yes	Nomimal
4	Yes	Nominal	No	Nominal
5	Yes	Nominal	Yes	Twice

TABLE V ECONOMIC PERFORMANCE FOR ALL CASES

Economic result	Case 1	Case 2	Case 3	Case 4	Case 5
Power system operation cost (\$)	22900	20400	13275	21472	28925
Gas system operation cost (\$)	15512	14485	12044	16324	26140
Water system operation cost (\$)	1962	1802	2310	1858	2352
System operation cost (\$)	40374	36687	27629	39609	57417

TABLE VI ECONOMIC PERFORMANCE FOR TWO STAGES

Economic result	Case 1	Case 2	Case 3	Case 4	Case 5
First-stage cost (\$)	32526	29520	22028	31087	47840
Expected Second-stage cost (\$)	7848	7167	5601	8522	9577
Total cost (\$)	40374	36687	27629	39609	57417

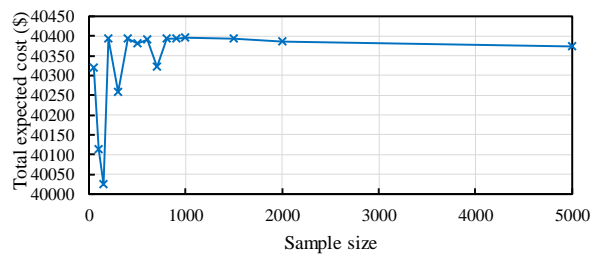


Fig. 3. Total expected cost of case 1 based on different sample size.

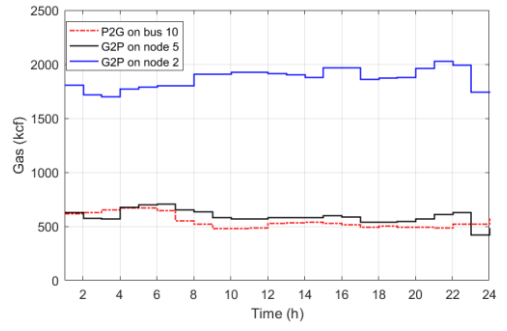


Fig. 4. Gas scheduling of gas turbines and P2G.

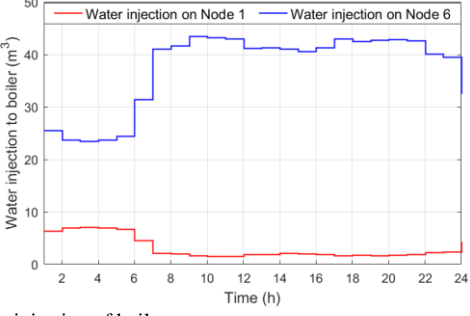


Fig. 5. Water injection of boilers.

consume more water with increasing renewable output. In case 4, there is no supply from the power system to the gas system, which causes the higher operation cost of gas system since the excessive renewable generation cannot be fully utilized. The operation cost of all the subsystems and the overall system is the highest in case 5. Compared with case 3 with the lowest cost, the total operation cost is 107% higher. Particularly, the gas system operation cost is \$26140, which is \$10628 more than that of case 1.

The IWENS operation cost of first and second stages are presented in TABLE VI. Case 5 results in the highest cost for both the first and second stages, i.e., \$47840 and \$9577. When the twice of the renewable generation capacity is considered, case 3 yields \$5601 of the adaptive recourse cost. In Fig. 3, the total expected IWENS operation cost with different number of simulation samples is given. The second-stage expected performance is conducted based on 1000 simulated uncertainty realizations. The sample size is changed to investigate its impact on second-stage operation cost. In Fig. 3, the result of case 1 fluctuates when the sample is fewer than 1000 and converges toward \$40374 afterwards.

B. Analysis of Energy Conversions

This section investigates the scheduling of coupling devices for interconnecting each system, i.e., gas turbines, P2G facility, electric boilers, CHP, gas furnace and GSHP. To begin with, the operation scheme of gas turbines and the P2G facility is given in Fig. 4. Note that it shows the input of gas turbines and output of P2G facility. It can be seen that the gas turbine at node 2 has higher gas consumption than node 5. The average gas consumption of node 2 is 1867kcf and that of node 5 is 591kcf. The potential reason of the higher gas consumption at node 2 are i) node 2 is connected to a natural gas source which has abundant gas supply and ii) the requirement of power transformation at bus 6 is higher as it is connected with more buses. As for P2G, it produces 549kcf averagely. The transformed gas from P2G can supply loads at nodes 3, 5 and 6. In addition, abundant gas can be converted back to the power system at node 5. The scheduling of

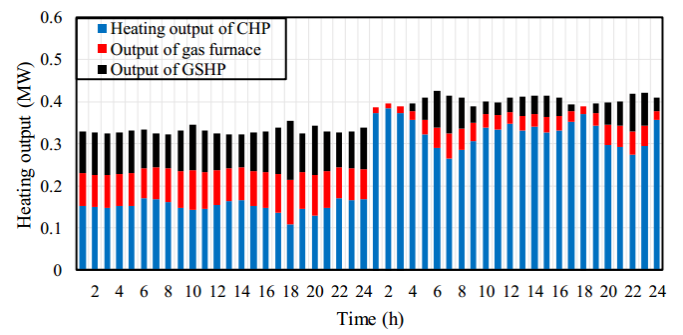


Fig. 6. Heating output of CHP, gas furnace and GSHP.

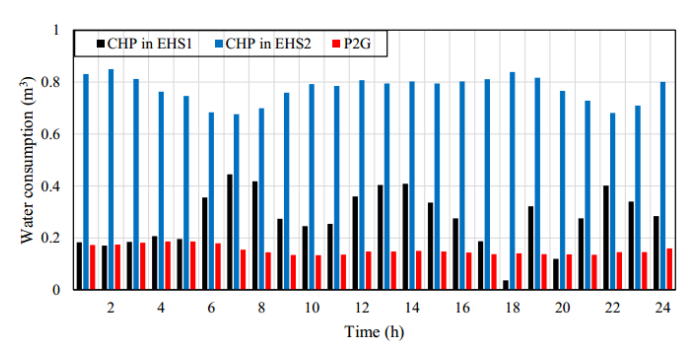


Fig. 7. Water consumption of CHPs and P2G.

water injection of electric boilers is shown in Fig. 5. The water injection is 3 at node 6m³ and 37 m³ at node 1 averagely. Although the heating loads of EHS 1 and 2 have similar amount, the heating supplied by water system at water node 1 is more than 6 times of that at node 6. Since the gas supply of EHS 2 connected to gas node 5 is less. However, the water supply from water node 1 is sufficiently connected to the water reservoir.

In Fig. 6, the heating output of converters in EHS 1 and 2 are given, respectively. Overall, the total heating output of converters in EHS 1 is 0.1MW higher than that of EHS 2. The heating supply composition is different for EHS 1 and 2. The CHP is utilized around 0.15MW for each hour and takes up 50% of the total heating output of converters. While the CHP in EHS 2 outputs approximately 0.33MW, which is 81% of the total heating conversion. The reason is that the supply from the power system is not sufficient, which affects the heat conversion of GSHP even though the heating conversion efficiency of GSHP is high. The insufficient electricity consumption needs to be satisfied by CHP conversion, which also increases heating conversion.

The water consumption of CHPs and P2G is in Fig. 7. As discussed for Fig. 6, the heating conversion from CHP in EHS 2 is higher than that of EHS 1. The water consumption of CHP in EHS 2 is also higher than that of EHS 1, i.e., the average water consumption of CHP in EHS 2 is 0.28m³ and it is 0.77 m³ of CHP in EHS 1. Compared to CHP, P2G consumes less water and its average water consumption is 0.15 m³.

C. The Impact of CVaR on Economic Performance

Through adjusting the confidence level and weighting factor for operation cost versus risk trade-off, the overall economic performance varies. TABLEs VII and VIII present the economic performance with different β and α , respectively. This paper considers 95% as the benchmark α used in TABLEs V and VI. As shown in TABLE VII, the total cost increases with the increase of α . For case 1, the highest total operation cost is \$40652 with β =0.9 and the lowest total operation cost is \$35635 with β =0.99. When β is fixed, case 5 which considers twice of

TABLE VII
ECONOMIC PERFORMANCE WITH DIFFERENT WEIGHTING FACTORS

Economic result (\$)	β =0.8	β=0.9	β=0.95	β=0.99
Case 1	35635	39573	40374	40652
Case 3	25830	26412	27629	27940
Case 4	38749	39015	39609	40527
Case 5	54119	57087	57417	57906

TABLE VIII
ECONOMIC PERFORMANCE WITH DIFFERENT CONFIDENCE LEVELS

Economic result (\$)	<i>α</i> =0	α=0.25	α=0.5	α=0.75
Case 1	36687	38200	40374	42049
Case 3	25872	26412	27629	28950
Case 4	37321	38580	39609	47140
Case 5	50767	51263	57417	62875

the original gas price has the highest total operation cost, followed by cases 4, 1 and 3, which is the same as discussed in section A. In TABLE VIII, the impact of changing β on the economic performance for all cases is presented. It can be seen that the higher α causes higher priority on minimizing the risk, which leads to higher operation cost. When α =0, the mean-risk DRO degrades into the risk-neutral DRO. For case 5, the total operation cost is only \$50767 compared with the \$57417 solved by the benchmark mean-risk DRO.

D. Result Discussion

This section presents the result discussion for sections A-C. The economic performance of all the cases is shown in TABLEs V-VI and Fig. 3. When CVaR is not considered in the objective function, there is a 10% reduction of the operation cost. The lowest operation cost is yielded when twice the capacity of renewable DGs is applied. Result also indicates that P2G connection does not have a profound impact on the economic performance. The twice of the gas generation price yields the highest operation cost, i.e., \$57417. In Fig. 3, the second-stage expected operation cost of case 1 shows that the computational result converges when the sample size is sufficiently large, i.e., 1000 samples. Based on different risk measure parameters, the economic performance is given in TABLEs VII and VIII. The results show that the higher confidence level and weighting coefficient lead to higher operation cost, e.g., the operation cost of case with β =0.99 is 14% higher than that with β =0.8.

The scheduling results of energy converters in Figs. 4-7 provide the system operator the guide for decision making. The converter scheduling of gas turbines, P2G facilities and boilers with water consumption are given in Figs. 4 and 5. Figs. 6 and 7 show that CHP is scheduled dominantly. GSHP with the highest conversion efficiency also presents a high utilization rate.

V. CONCLUSION

A mean-risk coordinated optimization for an IES in the waterenergy nexus with enormous interdependencies is proposed in this paper. The tight couplings and interactions between each subsystem enable the reliable and economic operation for the entire IES. The renewable uncertainty is captured by mean-risk DRO. The coherent risk measure, CVaR provides the trade-off to system operators with flexible alternatives on choosing between

[16]

IEEE TRANSACTIONS ON POWER SYSTEMS

economic efficiency and risk. A tractable Bender's decomposition is employed to solve the DR-IWENS problem. Through the extensive case studies on the economic performance, scheduling of interdependent coupling devices and the risk management via adjusting parameters, the major contributions are tested:

- The coordination of each subsystem with the conversion technologies enhances the energy efficiency of all vectors.
- The water system should be considered in the IES operation as water is extensively consumed by energy conversions.
- The mean-risk DRO applied in IES operation problem provides system operators with not only economic but risk concerns.

This work provides system operators a two-stage operation scheme to minimise system operation cost while dealing with enormous cross energy vector interdependencies, thus helping lowering utility bills for end customers.

The future work aims to resolve two problems: i) a more practical decentralized operation mechanism will be considered, i.e., power, gas and water subsystems are owned by independent system operators, and ii) a complete heating network will be modelled in the IWENS, which will further enhance the energy efficiency for the system with more supply flexibility for energy hubs.

REFERENCES

- [1] P. Zhao et al., "Economic-Effective Multi-Energy Management with Voltage Regulation Networked with Energy Hubs," *IEEE Transactions on Power Systems*, pp. 1-1, 2020, doi: 10.1109/TPWRS.2020.3025861.
- [2] E. A. M. Ceseña and P. Mancarella, "Energy Systems Integration in Smart Districts: Robust Optimisation of Multi-Energy Flows in Integrated Electricity, Heat and Gas Networks," *IEEE Transactions on Smart Grid*, vol. 10, no. 1, pp. 1122-1131, 2019, doi: 10.1109/TSG.2018.2828146.
- [3] D. Huo, C. Gu, K. Ma, W. Wei, Y. Xiang, and S. L. Blond, "Chance-Constrained Optimization for Multienergy Hub Systems in a Smart City," *IEEE Transactions on Industrial Electronics*, vol. 66, no. 2, pp. 1402-1412, 2019, doi: 10.1109/TIE.2018.2863197.
- [4] D. Huo, S. Le Blond, C. Gu, W. Wei, and D. Yu, "Optimal operation of interconnected energy hubs by using decomposed hybrid particle swarm and interior-point approach," *International Journal of Electrical Power & Energy Systems*, vol. 95, pp. 36-46, 2018/02/01/ 2018, doi: https://doi.org/10.1016/j.ijepes.2017.08.004
 [5] H. Wang, C. Gu, Y. Zheng, E. V. Jank, C. W. J. Wang, C. Gu, Y. Zheng, E. V. Jank, C. W. J. Wang, C. Gu, Y. Zheng, E. V. Jank, C. W. J. Wang, C. Gu, Y. Zheng, E. V. Jank, C. W. J. Wang, C. Gu, Y. Zheng, E. V. Jank, C. W. J. Wang, C. Gu, Y. Zheng, E. V. Jank, C. W. J. Wang, C. Gu, Y. Zheng, E. V. Jank, C. W. J. Wang, C. Gu, Y. Zheng, E. V. Jank, C. W. J. Wang, C. Gu, Y. Zheng, E. V. Jank, C. W. Wang, C. Gu, Y. Zheng, E. V. Jank, C. W. Wang, C. Gu, Y. Zheng, E. V. Jank, C. W. Wang, C. Gu, Y. Zheng, E. V. Jank, C. W. Wang, C. Gu, Y. Zheng, E. V. Jank, C. W. Wang, C. Gu, Y. Zheng, E. V. Jank, C. W. Wang, C. W. Zheng, E. V. Jank, C. W. Wang, C. W. Zheng, E. V. Jank, C. W. Wang, C. W. Wang, C. W. Zheng, E. V. Jank, C. W. Wang, C. W. Wang, C. W. Zheng, E. V. Jank, C. W. Wang, C. W. Zheng, E. V. Zheng, E. V. Jank, C. W. Wang, C. W. Zheng, E. V. Zheng, E. V. Jank, C. W. Wang, C. W. Zheng, E. V. Zheng, E. V. Zheng, E. V. Jank, C. W. Wang, C. W. Zheng, E. V. Zheng, E
- [5] H. Wang, C. Gu, X. Zhang, F. Li, and L. Gu, "Identifying the correlation between ambient temperature and gas consumption in a local energy system," *CSEE Journal of Power and Energy Systems*, vol. 4, no. 4, pp. 479-486, 2018, doi: 10.17775/CSEEJPES.2017.00260.
- [6] S. Shin et al., "A systematic review of quantitative resilience measures for water infrastructure systems," Water, vol. 10, no. 2, p. 164, 2018.
- [7] V. M. Leiby and M. E. Burke, Energy efficiency best practices for North American drinking water utilities. WRF, 2011.
- [8] A. S. Zamzam, E. Dall'Anese, C. Zhao, J. A. Taylor, and N. D. Sidiropoulos, "Optimal Water–Power Flow-Problem: Formulation and Distributed Optimal Solution," *IEEE Transactions on Control of Network Systems*, vol. 6, no. 1, pp. 37-47, 2019, doi: 10.1109/TCNS.2018.2792699.
- [9] K. Oikonomou and M. Parvania, "Optimal Coordination of Water Distribution Energy Flexibility With Power Systems Operation," *IEEE Transactions on Smart Grid*, vol. 10, no. 1, pp. 1101-1110, 2019, doi: 10.1109/TSG.2018.2824308.
- [10] Q. Li, S. Yu, A. S. Al-Sumaiti, and K. Turitsyn, "Micro Water–Energy Nexus: Optimal Demand-Side Management and Quasi-Convex Hull Relaxation," *IEEE Transactions on Control of Network Systems*, vol. 6, no. 4, pp. 1313-1322, 2019, doi: 10.1109/TCNS.2018.2889001.
- [11] L. Ji, B. Zhang, G. Huang, and P. Wang, "A novel multi-stage fuzzy stochastic programming for electricity system structure optimization and planning with energy-water nexus A case study of Tianjin, China," *Energy*, vol. 190, p. 116418, 2020/01/01/2020, doi: https://doi.org/10.1016/j.energy.2019.116418.
- [12] Y. Li, Z. Li, F. Wen, and M. Shahidehpour, "Minimax-Regret Robust Co-Optimization for Enhancing the Resilience of Integrated Power Distribution and Natural Gas Systems," *IEEE Transactions on Sustainable Energy*, vol. 11, no. 1, pp. 61-71, 2020, doi: 10.1109/TSTE.2018.2883718.
- B. Zhou et al., "Optimal Scheduling of Biogas—Solar—Wind Renewable Portfolio for Multicarrier Energy Supplies," *IEEE Transactions on Power Systems*, vol. 33, no. 6, pp. 6229-6239, 2018, doi: 10.1109/TPWRS.2018.2833496.
- [14] P. Zhao, C. Gu, Z. Hu, X. I. E. D, I. Hernando-Gil, and Y. Shen, "Distributionally Robust Hydrogen Optimization with Ensured Security and Multi-Energy

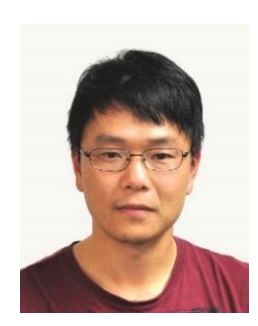
- Couplings," IEEE Transactions on Power Systems, pp. 1-1, 2020, doi: 10.1109/TPWRS.2020.3005991.
- [15] F. Qi, M. Shahidehpour, F. Wen, Z. Li, Y. He, and M. Yan, "Decentralized Privacy-Preserving Operation of Multi-Area Integrated Electricity and Natural Gas Systems with Renewable Energy Resources," *IEEE Transactions on Sustainable Energy*, pp. 1-1, 2019, doi: 10.1109/TSTE.2019.2940624.
 - F. Liu, Z. Bie, and X. Wang, "Day-Ahead Dispatch of Integrated Electricity and Natural Gas System Considering Reserve Scheduling and Renewable Uncertainties," *IEEE Transactions on Sustainable Energy*, vol. 10, no. 2, pp. 646-658, 2019, doi: 10.1109/TSTE.2018.2843121.
- [17] P. Zhao et al., "Volt-VAR-Pressure Optimization of Integrated Energy Systems with Hydrogen Injection," *IEEE Transactions on Power Systems*, pp. 1-1, 2020, doi: 10.1109/TPWRS.2020.3028530.
- [18] L. Wu, C. He, X. Zhang, and T. Liu, "Distributionally Robust Scheduling of Integrated Gas-Electricity Systems with Demand Response," *IEEE Transactions* on Power Systems, pp. 1-1, 2019, doi: 10.1109/TPWRS.2019.2907170.
- [19] X. Lu, K. W. Chan, S. Xia, X. Zhang, G. Wang, and F. Li, "A Model to Mitigate Forecast Uncertainties in Distribution Systems Using the Temporal Flexibility of EVAs," *IEEE Transactions on Power Systems*, vol. 35, no. 3, pp. 2212-2221, 2020, doi: 10.1109/TPWRS.2019.2951108.
- [20] P. Zhao, C. Gu, and D. Huo, "Two-Stage Coordinated Risk Mitigation Strategy for Integrated Electricity and Gas Systems under Malicious False Data Injections," *IEEE Transactions on Power Systems*, pp. 1-1, 2020, doi: 10.1109/TPWRS.2020.2986455.
- [21] Y. Chen, Q. Guo, H. Sun, Z. Li, W. Wu, and Z. Li, "A Distributionally Robust Optimization Model for Unit Commitment Based on Kullback–Leibler Divergence," *IEEE Transactions on Power Systems*, vol. 33, no. 5, pp. 5147-5160, 2018, doi: 10.1109/TPWRS.2018.2797069.
- [22] Z. Li, W. Wu, B. Zhang, and X. Tai, "Kullback–Leibler divergence-based distributionally robust optimisation model for heat pump day-ahead operational schedule to improve PV integration," *IET Generation, Transmission & Distribution*, vol. 12, no. 13, pp. 3136-3144, 2018, doi: 10.1049/iet-gtd.2017.2062.
- [23] M. Asensio and J. Contreras, "Stochastic Unit Commitment in Isolated Systems With Renewable Penetration Under CVaR Assessment," *IEEE Transactions on Smart Grid*, vol. 7, no. 3, pp. 1356-1367, 2016, doi: 10.1109/TSG.2015.2469134.
- [24] C. Peng, Y. Hou, N. Yu, and W. Wang, "Risk-Limiting Unit Commitment in Smart Grid With Intelligent Periphery," *IEEE Transactions on Power Systems*, vol. 32, no. 6, pp. 4696-4707, 2017, doi: 10.1109/TPWRS.2017.2672939.
- [25] L. Yang, J. Jian, Y. Xu, Z. Dong, and G. Ma, "Multiple Perspective-Cuts Outer Approximation Method for Risk-Averse Operational Planning of Regional Energy Service Providers," *IEEE Transactions on Industrial Informatics*, vol. 13, no. 5, pp. 2606-2619, 2017, doi: 10.1109/TII.2017.2710055.
- [26] S. Li, H. He, C. Su, and P. Zhao, "Data driven battery modeling and management method with aging phenomenon considered," *Applied Energy*, vol. 275, p. 115340, 2020/10/01/ 2020, doi: https://doi.org/10.1016/j.apenergy.2020.115340.
- [27] S. Li, H. He, and J. Li, "Big data driven lithium-ion battery modeling method based on SDAE-ELM algorithm and data pre-processing technology," Applied Energy, vol. 242, pp. 1259-1273, 2019/05/15/ 2019, doi: https://doi.org/10.1016/j.apenergy.2019.03.154.
- [28] H. Yeh, D. F. Gayme, and S. H. Low, "Adaptive VAR Control for Distribution Circuits With Photovoltaic Generators," *IEEE Transactions on Power Systems*, vol. 27, no. 3, pp. 1656-1663, 2012, doi: 10.1109/TPWRS.2012.2183151.
- [29] B. Wang, C. Zhang, and Z. Dong, "Interval Optimization Based Coordination of Demand Response and Battery Energy Storage System Considering SoC Management in A Microgrid," *IEEE Transactions on Sustainable Energy*, pp. 1-1, 2020, doi: 10.1109/TSTE.2020.2982205.
- [30] S. Doan, H. Yeh, and Y. Yang, "Two-Mode Adaptive Schemes for VAR Control With Solar Power and Energy Storage," *IEEE Systems Journal*, vol. 14, no. 1, pp. 889-899, 2020, doi: 10.1109/JSYST.2019.2920016.
- [31] T. Haktanır and M. Ardıçlıoğlu, "Numerical modeling of Darcy-Weisbach friction factor and branching pipes problem," *Advances in Engineering Software*, vol. 35, no. 12, pp. 773-779, 2004.
- [32] A. Buttler and H. Spliethoff, "Current status of water electrolysis for energy storage, grid balancing and sector coupling via power-to-gas and power-toliquids: A review," *Renewable and Sustainable Energy Reviews*, vol. 82, pp. 2440-2454, 2018.
- [33] L. Liu, L. Fu, and Y. Jiang, "Application of an exhaust heat recovery system for domestic hot water," *Energy*, vol. 35, no. 3, pp. 1476-1481, 2010.
- [34] X. Lu, K. W. Chan, S. Xia, B. Zhou, and X. Luo, "Security-Constrained Multiperiod Economic Dispatch With Renewable Energy Utilizing Distributionally Robust Optimization," *IEEE Transactions on Sustainable Energy*, vol. 10, no. 2, pp. 768-779, 2019, doi: 10.1109/TSTE.2018.2847419.
 [35] R. T. Rockafellar and S. Uryasev, "Optimization of conditional value-at-risk,"
- [35] R. T. Rockafellar and S. Uryasev, "Optimization of conditional value-at-risk," *Journal of risk*, vol. 2, pp. 21-42, 2000.
 [36] S. Zhu and M. Fukushima, "Worst-case conditional value-at-risk with
- [36] S. Zhu and M. Fukushima, "Worst-case conditional value-at-risk with application to robust portfolio management," *Operations research*, vol. 57, no. 5, pp. 1155-1168, 2009.
- [37] S. Dempe, "Directional differentiability of optimal solutions under Slater's condition," *Mathematical Programming*, vol. 59, no. 1-3, pp. 49-69, 1993.
- [38] A. Ruszczyński and A. Shapiro, "Optimality and duality in stochastic programming," *Handbooks in Operations Research and Management Science*, vol. 10, pp. 65-139, 2003.
- [39] P. Zhao, C. Gu, D. Huo, Y. Shen, and I. Hernando-Gil, "Two-Stage Distributionally Robust Optimization for Energy Hub Systems," *IEEE*

Transactions on Industrial Informatics, vol. 16, no. 5, pp. 3460-3469, 2020, doi: 10.1109/TII.2019.2938444.



Pengfei Zhao (S'18) was born in Beijing, China. He received the double B.Eng. degree from the University of Bath, U.K., and North China Electric Power University, Baoding, China, in 2017. He received the Ph.D degree from the University of Bath, U.K. He was a visiting Ph.D. student at Smart Grid Operations and Optimization Laboratory (SGOOL), Tsinghua University, Beijing, China in 2019. He is currently an Assistant Professor at the State Key Laboratory of Management and Control for Complex Systems, Institute of Automation, Chinese Academy of Sciences. His major research

interests include the intelligent decision-making of complex energy systems and public health big data.



Chenghong Gu (M'14) was born in Anhui province, China. He received the Master's degree from the Shanghai Jiao Tong University, Shanghai, China, in 2007 in electrical engineering. He received the Ph.D. degree from the University of Bath, U.K. He is currently a Lecturer and EPSRC Fellow with the Department of Electronic and Electrical Engineering, University of Bath. His major research interest is in multi-vector energy system, smart grid, and power economics.



Zhidong Cao is an Associate Professor at the State Key Laboratory of Management and Control for Complex Systems, Institute of Automation, Chinese Academy of Sciences. His research interests include public health big data and infectious disease informatics.



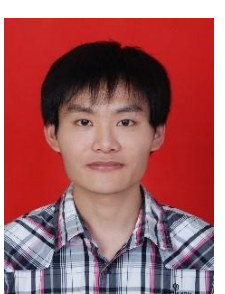
Qian Ai (Senior Member, IEEE) received the bachelor's degree in electrical engineering from Shanghai Jiao Tong University, Shanghai, China, in 1991, the master's degree in electrical engineering from Wuhan University, Wuhan, China, in 1994, and the Ph.D. degree in electrical engineering from Tsinghua University, Beijing, China, in 1999. He was with Nanyang Technological University, Singapore, for one year and the University of Bath, Bath, U.K., for two years. He was with Shanghai Jiao Tong University, where he is currently a Professor with the School of Electronic Information and Electrical Engineering. His current research interests include power quality, load modeling, smart grids,

microgrid, and intelligent algorithms. He was a recipient of the IEEE Industrial Application Society Prize Paper Award in 2016.



Yue Xiang (SM'20) received the B.S. and Ph.D. degrees from Sichuan University, China, in 2010 and 2016, respectively. From 2013 to 2014, he was a joint Ph.D. student at the Department of Electrical Engineering and Computer Science, University of Tennessee, Knoxville, US, a visiting scholar at the Department of Electronic and Electrical Engineering, University of Bath, UK in 2015, and also a visiting researcher at Department of Electronic Engineering, Imperial College London, UK in 2019-2020. Now he is an associate professor in the College

of Electrical Engineering, Sichuan University, China. His main research interests are distribution network planning and optimal operation, power economics, electric vehicle integration and smart grids.



Tao Ding (SM'19) received the Ph.D. degree from Tsinghua University, Beijing, China, in 2015. During 2013 and 2014, he was a Visiting Scholar in the Department of Electrical Engineering and Computer Science, University of Tennessee, Knoxville, TN, USA. During 2019 and 2020, he was a Visiting Scholar in the Department of Electrical Engineering and Computer Science, Illinois Institute of Technology, Chicago, IL, USA. He is currently a Professor in the School of Electrical Engineering, Xi'an Jiaotong University. His current research interests include electricity markets, power system economics and

optimization methods. He has published more than 100 technical papers and authored by "Springer Theses" recognizing outstanding Ph.D. research around the world and across the physical sciences—Power System Operation with Large Scale Stochastic Wind Power Integration. He received the excellent doctoral dissertation from Tsinghua University, and Outstanding Graduate Award of Beijing City. Dr. Ding is an Editor of IEEE Transactions on Power Systems, IET Generation Transmission& Distribution.



Xi Lu received the B.Eng. degree in Electrical Engineering from North China Electric Power University, Beijing, China in 2015. He is currently pursuing the PhD degree in Electrical Engineering at the Hong Kong Polytechnic University, Hong Kong, China. His research interests include dispatch of electric vehicle aggregators, distribution system operation and applications of robust optimization and distributionally robust optimization in power systems, etc.



Xinlei Chen is currently a postdoctoral research associate in Electrical Engineering Department at Carnegie Mellon University. He received the B.E. and M.S. degrees in Electronic Engineering from Tsinghua University, China, in 2009 and 2012, respectively, and Ph.D degrees in Electrical Engineering from Carnegie Mellon University, Pittsburgh, PA, USA. His research interests lie in mobile computing, crowd intelligence, cyber physical system, mobile embedded system etc.





Shuangqi Li was born in Beijing, China. He received the B.Eng. degree in vehicle engineering from Beijing Institute of Technology, Beijing, China, in 2018. He worked as a research assistant at the National Engineering Laboratory for Electric Vehicles, Beijing Institute of Technology from 2018 to 2019. Currently, he is pursuing the Ph.D. degree at the Department of Electronic and Electrical Engineering, University of Bath. His major research interest is the big data analysis, deep-learning algorithm, operation and planning of smart grid system and V2G service.